Proc. Schl. Eng. Tokai Univ., Ser. E
41 (2016) 39-46

Structural Characteristics of New Concrete Filled Steel I-Girder

by

Waheed Ahmad SAFI[*1] and Shunichi NAKAMURA[*2]

(Received on Mar. 30, 2016 and accepted on May 12, 2016)

Abstract

In the continuous plate girder bridge with steel I-section and RC slab, the critical section is always at the intermediate support where the bending moment is maximum and the concrete slab does not contribute. A new structural solution is proposed: concrete is filled in the area surrounded by the upper and lower flanges and the web. The filled concrete contributes and restricts the local buckling of the flange and the web. Experiments showed that the bending strength of the concrete filled steel I-section was 2.5 times larger than the conventional one and the shear strength was 3.0 times. A trial design was carried out for a four-span continuous plate girder bridge with concrete filled steel I-section and was compared with the conventional plate girder bridge. The thickness of the flanges and web can be less than 70 % at the intermediate support and 20 % at the span center. It is verified that the proposed concrete filled steel I-section is feasible and economical.

Keywords: Concrete filled steel I-girder, Steel I-girder, Limit state design, Bending strength, Shear strength

1. Introduction

The steel I-girders are the simplest and the most commonly used structures for short to medium span bridges. For a simply supported bridge the composite girder consisting of the steel I-girder and the concrete slab is ideal. The lower part of the girder section is in tension which can be resisted by the steel girder and the upper part is in compression which is resisted by the RC slab. It is connected to the top of upper flanges with shear studs. For a continuous girder bridge the bending moment is positive at the span center and negative at the intermediate support. At the mid-span the steel/concrete composite girder is ideal: the steel and concrete sections resist tensile and compressive forces respectively. On the other hand, as large negative bending moments and shear forces exist at the intermediate supports; the concrete slab is in tension and does not contribute to resist the negative bending moment. As the lower flanges and lower parts of webs are in compression and vulnerable to lateral-torsional buckling, the lower flange is wider and thicker.

In addition, the web is also thicker and stiffened by vertical and horizontal stiffeners, which increases the total cost of the bridge. Thus, the area around the intermediate support is the most critical part of the continuous steel plate girder bridges. In order to improve and strengthen structural performance and behaviour of continuous steel I-girder bridges under negative bending moment at the intermediate support, the area surrounded by the flanges and the web is filled with concrete. This CFIG (Concrete filled I-girder) was proposed for the intermediate support area[1)]. The filled concrete in the compression zone contributes to bending strength and also restricts the local buckling of the lower flange and web; resulting in economical steel sections compared with the conventional continuous plate girder bridge (CCG) (Fig.3). Furthermore, steel reinforcing bars are placed in the filled concrete region (Fig.1, Fig.2) to restrict concrete falling down from the web and strengthen the web. This form was experimentally tested and proved by Nakamura[2)] which can be applied at the intermediate support of composite steel girder bridges.

In this study, an analytical method was developed to calculate the bending strength of the CFIG girder. Then, a trial design was also carried out for the four-span continuous

*1 Graduate student, Course of Civil Engineering.
*2 Professor, Department of Civil Engineering

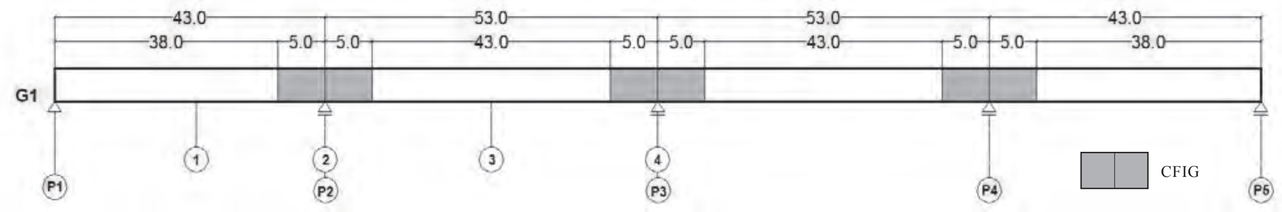

Fig.1 Longitudinal view of Concrete filled I-Girder (CFIG) bridge (unit: m)

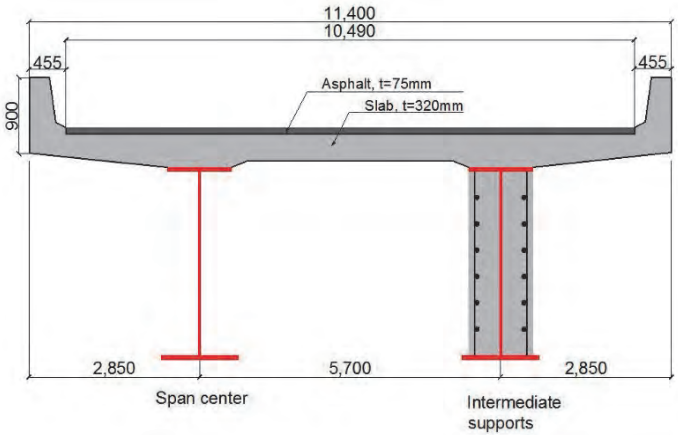

Fig.2 Cross section of Concrete filled I-Girder (CFIG) bridge (unit: mm)

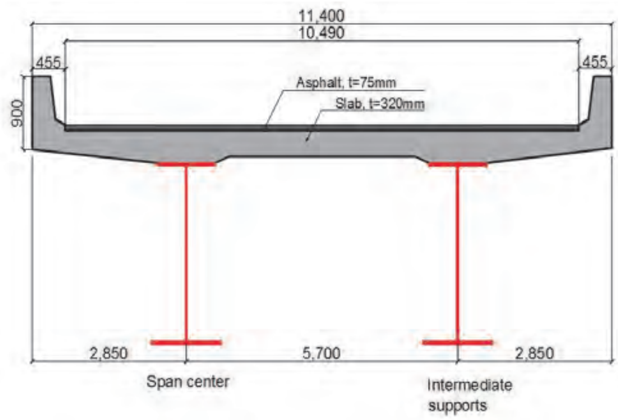

Fig.3 Cross section of Conventional I-Girder (CCG) bridge (unit: mm)

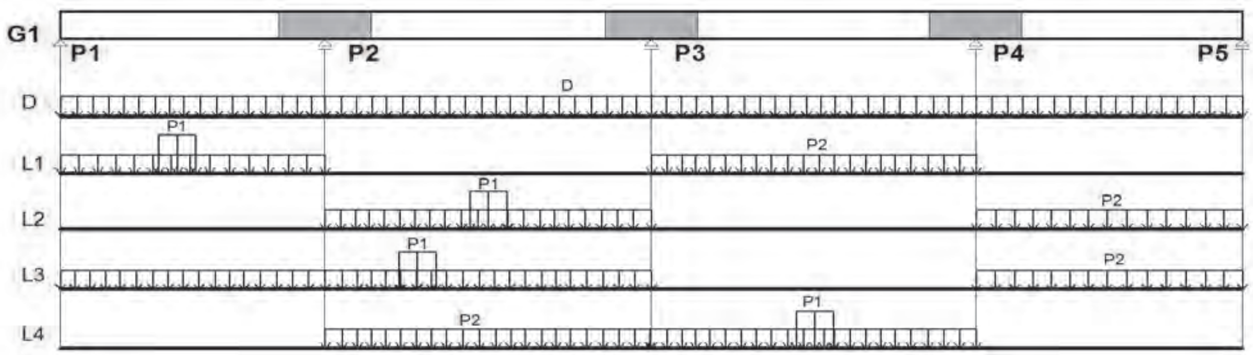

Fig.4 Design load cases

composite steel I-girder highway bridge. The result with CFIG was compared with CCG (conventional steel/concrete composite I-girder), which is expected to show advantages of CFIG. Basic structural behavior and strength of CFIG was also clarified by the experiments.

2. Trial Design

A trial design was carried out for the four-span continuous girder bridge. The bridge has 4 spans (43+2@53+43m) with a total width of 11.4m (Fig.1). In this study two types of models were compared: Model I is a concrete filled steel I-girder (CFIG) and Model II the conventional steel/concrete composite I-girder (CCG). The material and sectional properties of steel are assumed for this study is shown in Table 1. (CCG) is a conventional steel I-girder and (CFIG) is a concrete filled steel I-girder with steel reinforcements inside the filled concrete. This bridge model was chosen from the Guidelines for performance verification of steel–concrete hybrid structures (Japanese Association of Civil Engineers, 2006). The cross section of the girder is shown in Fig.2 and Fig.3. The reinforcing bars with 16mm in diameter were placed vertically and horizontally at the interval of 450mm and 300mm respectively inside the CFIG area.

2.1 *Design loads*

The design loads consist of the pre-composite dead load (D1) due to the self-weight of girder, formworks and concrete slab and the post-composite dead load (D2) due to the surface wearing, railings of the bridge and live load (L). The design live load consists of equivalent concentrated load (P1=3.5kN/m^2) with the longitudinal width of 10m and fully uniformly distributed load (P2=10.0kN/m^2). These design live loads conform to the Japanese specification for highway bridges[3)]. Four critical cases for the live load (L_1, L_2, L_3 and

L_4) are considered for both CFIG and CCG girders (Fig.4). L_1 is applied at 19 m from the first support produced maximum bending moment effects on the first mid-span, L_3 is applied at the alternate spans of the girders produced maximum bending effects on the second intermediate support and L_4 is applied on the two intermediate spans of the girder; resulting maximum bending moment effects on the third support which is more critical than L_1, L_2 and L_3.

2.2 *Sectional forces*

Structural analysis was conducted for CFIG and CCG Models by a structural analysis program (CSI SAP2000, v16). Fig.5 shows the design bending moment due to dead load (D) and the maximum and minimum bending moment due to live loads (L_1-L_4) for CFIG Model. It is understood that the negative bending moment is critical at the intermediate supports and the positive bending moment is critical at the span centers.

The material behavior of the steel was represented by the tri-linear stress-strain curve shown in Fig.6. The yield strength fsy, yield strain εsy and the ultimate strength fsu need to be define to the stress–strain curve, while the strain at the onset of strain hardening εst and the ultimate strain limit εsu were assumed to be 0.02 and 0.08 respectively. For the steel reinforcement a simpler elastic–perfectly plastic model without strain hardening behavior is considered. The non-linear behavior of the concrete material is used by equivalent uniaxial stress-strain curve as shown in Fig.7. For the concrete in compression, material properties are required to fulfill the behavior of the slab and filled concrete inside steel plate section.

The stress-strain curve, based on the equations (1, 2, 3 & 4), which is provided in the JSCE code specification is used for the compressive behavior of concrete. At the peak stress εco is considered as εco=0.002 and the ultimate strain is taken as εcu=0.0035. Where σ_c: is the compressive strength of concrete, f_{ck}: is the nominal compressive strength and ε_c is the concrete strain.

$$\sigma_c = 0.85 f_{ck}\left(\frac{\varepsilon_c}{0.002}\right)\left\{2-\left(\frac{\varepsilon_c}{0.002}\right)\right\}, \quad (\varepsilon_c \le 0.002) \tag{1}$$

$$\sigma_c = 0.85 f_{ck}, \qquad (\varepsilon_c > 0.002) \tag{2}$$

$$k_1 = 1 - 0.003 f_{ck}, \quad (k_1 \le 0.002) \tag{3}$$

$$\varepsilon_{cu} = \left(155 - \frac{f_{ck}}{3000}\right), \ (\varepsilon_{cu} > 0.0035) \tag{4}$$

2.3 *Safety verification*

Table 1 shows the assumed cross-section of the girder at the mid-span and intermediate support. The SM490YB (tensile strength of 490MPa) steel grade is used at the mid-span and intermediate support of CFIG and CCG girders.

Table 2 shows the safety verification for the pre-composite section of CFIG and CCG girders. The verification method conforms to "Guidelines for performance verification of steel–concrete hybrid structures[4)]". The design bending moment due to pre-composite dead loads (M_{d1}) is within the resisting capacity of the steel girder (M_{sud}).

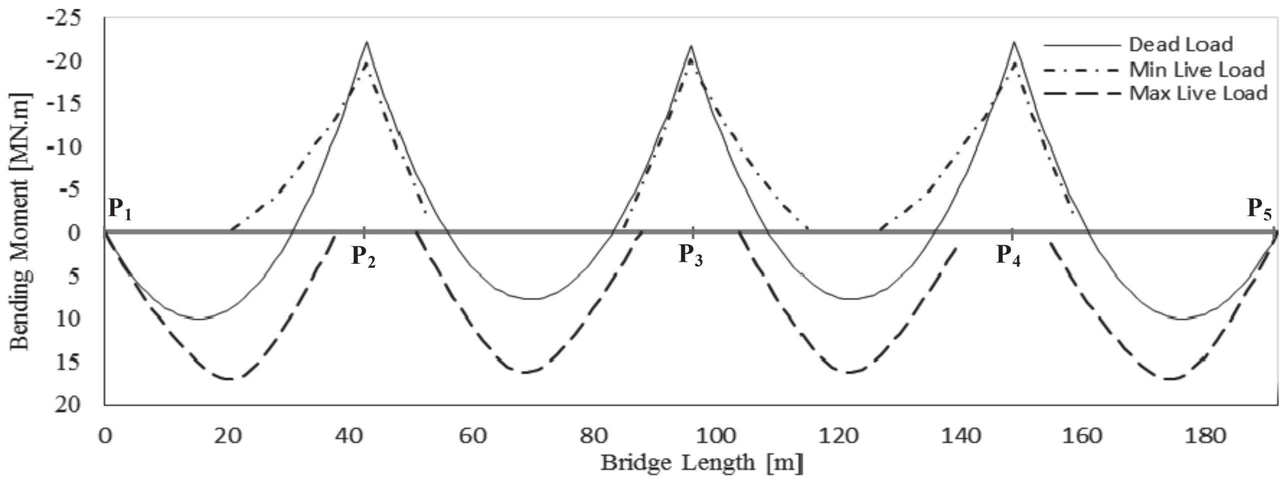

Fig.5 Design bending moment

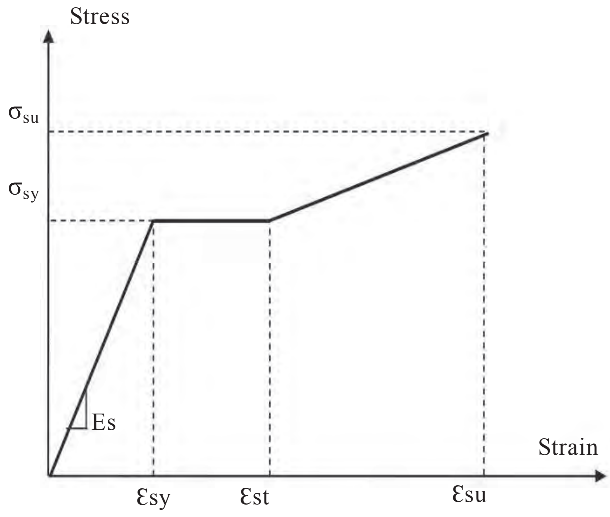

Fig.6 Stress-strain relation for the steel.

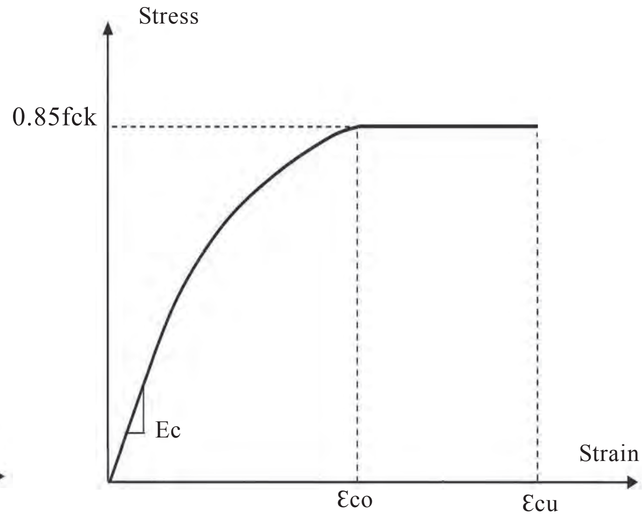

Fig.7 Stress-strain relation for the concrete.

Table 1 Sectional properties of CFIG & CCG models

Bridge girder system		Concrete Filled I-girder(CFIG)				Conventional I-girder (CCG)			
Section(mm) *Steel grade*		SEC 1 *SM490YB*	SEC 2 *SM490YB*	SEC 3 *SM490YB*	SEC 4 *SM490YB*	SEC 1 *SM490YB*	SEC 2 *SM490YB*	SEC 3 *SM490YB*	SEC 4 *SM490YB*
Upper Flange	Width	400	500	400	500	500	700	500	700
	Thickness	18	25	17	25	19	35	18	35
Web	Height	2860	2845	2861	2843	2852	2816	2854	2816
	Thickness	14	15	14	17	13	16	13	16
Lower flange	Width	700	600	500	600	800	800	800	800
	Thickness	22	30	22	32	29	49	28	49
Cross sectional area (mm^2)		62,640	73,175	57,854	80,031	69,776	108,756	68,502	108,756
		(0.9)	(0.67)	(0.84)	(0.73)	(1.0)	(1.0)	(1.0)	(1.0)

Table 2 Safety check for the pre-composite section of CFIG and CCG girders

Section	Model	Design Bending Moment $1.1M_{d1}$	Design Bending Moment Capacity $M_{sud,t}$	$M_{sud,c}$	$(1.1M_{d1}/M_{sud})*Y_i \leq 1$ T-Side	C-Side
Section 1	CCG	7,456	22,918	8,521	0.36	0.96
Section 2	CCG	-14,439	24,624	-21,320	0.65	0.74
Section 3	CCG	6,310	21,983	7,832	0.31	0.89
Section 4	CCG	-14,650	-50,504	-43,726	0.32	0.37
Section 1	CFIG	7,057	17,979	7,778	0.43	1.00
Section 2	CFIG	-15,544	33,480	-24,643	0.51	0.69
Section 3	CFIG	5,487	15,341	6,676	0.39	0.90
Section 4	CFIG	-15,194	-39,050	-26,161	0.43	0.64

Fig.8 (a) shows the stress distribution of the section at the ultimate stage of CFIG at the intermediate support subjected to negative bending moment and the neutral axis lies within the web. In addition, the compressive forces at the lower part is resisted by the steel girder, reinforcing bars and filled concrete within the web and flanges. The tensile forces at the upper part are resisted by the reinforcing bars and the upper part of the steel plate girder. Fig.8 (b) shows the stress distribution at the span center subjected to positive bending moment. The neutral axis lies within the concrete slab due to thinner thickness of concrete slab. The lower part below the neutral axis is tension which is resisted by the steel girder. The upper part is in compression which is resisted by concrete slab.

Table 3 shows the safety verification for the post-composite section. The load factors and the structure factor (Υ_i) conform to the "Guidelines for performance verification of steel–concrete hybrid structures[4)]". The design bending moments (M_d) is within the resistance bending moment capacity (M_{ud}), which confirms that the assumed cross section is appropriate and safe. It is found from this trial design that the thickness of the flanges and web of CFIG can be less than 70 % of CCG at the intermediate support. Also, those of CFIG can be less than 10 % at the span center.

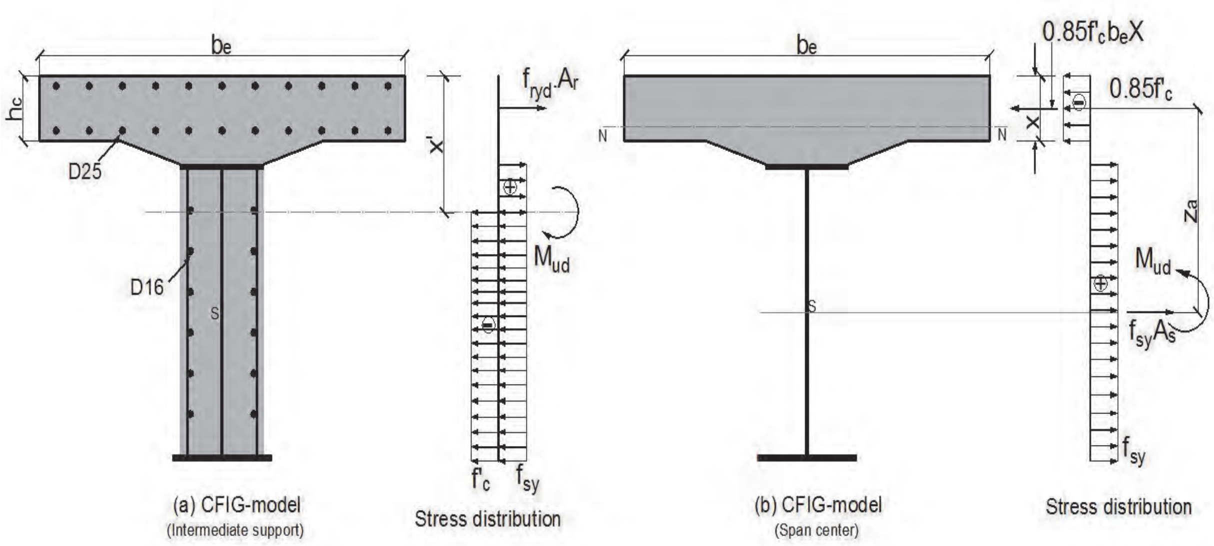

Fig.8 Stress distribution of the CFIG girders

Table 3 Safety check for the post-composite section of CFIG and CCG girders

Section			Section 1	Section 2	Section 3	Section 4
Pre-Composite Dead Load	$1.1M_{d1}$	CCG girder	7,456	-14439	6,310	-14,650
Post-Composite Dead load	$1.2M_{d2}$		3,164	-6,124	2,686	-6,200
Live load	1.98L		17,103	-17,660	17,452	-18,452
Design Bending Moment	M_d [kN.m]		27,723	-38,223	26,448	-39,302
Resistance Bending moment	M_{ud} [kN.m]		43,863	61,500	43,050	61,500
Pre-Composite Dead Load	$1.1M_{d1}$	CFIG girder	7,057	-15,544	5,487	-15,194
Post-Composite Dead load	$1.2M_{d2}$		2,958	-6,690	2,285	-6,436
Live load	1.98L		17,109	-19,602	16,327	-20,117
Design Bending Moment	M_d [kN.m]		27,124	-41,836	24,098	-41,747
Resistance Bending moment	M_{ud} [kN.m]		53,461	62,756	47,366	67,415
ϒi		1.1				
ϒi*Md/Mud≤1.0		CCG	0.70	0.68	0.68	0.70
		CFIG	0.56	0.73	0.56	0.68

3. Bending Test

3.1 *Test method and specimen*

Bending tests were performed with three type of models (Fig.9). The model BS was the steel plate girder. The web was 900 mm high and 6 mm thick, and the flanges were 200 mm wide and 12 mm thick. The web was stiffened by intermediate vertical stiffeners at interval of 375 mm and the models were laterally restrained from lateral movements at the support. The BC model is the concrete encased girder. The steel reinforcing bars with 10 mm in diameter were places vertically at intervals of 200 mm and welded to the upper and lower flanges and the horizontal reinforcing bars were also placed horizontally and connected with vertical bars by wires.

The BC-N had the same dimension as BC but the vertical reinforcing bars were not welded to the upper and lower flanges of the steel plate girder. The symbol N stands for the non-welding. The fabrication for the BC-N model is easier than BC model but the confined effects of concrete becomes smaller. On the other hand, the fatigue problem may occurs at the welded parts and it can be avoided in the non-welded model. The BC-N had the same dimension as BC but the vertical reinforcing bars were not welded to the upper and lower flanges of the steel plate girder. The symbol N stands for the non-welding. The fabrication for the BC-N model is easier than BC model but the confined effects of concrete becomes smaller. On the other hand, the fatigue problems may occur at the welded parts and it can be avoided in the non-welded model.

The steel plate I-girder was placed flat and then poured with concrete to the one side after other by concrete hardened. This encased composite girder is expected to be not only useful for new girders but also useful for repair and rehabilitation of the damaged or old girders. The steel I-girders of these two models had the same dimensions and were fabricated from the same steel plate.

3.2. *Test result*

Fig.10 shows a relation of the applied load vs. measured vertical displacements at mid-span. The applied load first increased linearly, reached the maximum point and then collapsed when the web and upper flange buckled in the BS model. In the BC model the applied load increased sharper than BS and in the linear part and the relation becomes non-linear after the compressive flange buckled.

The result for the non-welded model BC-N was between BS and BC models. The maximum load was almost 15 % lower than that of BC model because of confined effects of encased concrete; although, it was 1.5 times higher than that of the steel model BS. However, the girder showed a good ductile property. It is noted that the maximum bending strength of the filled concrete model BC was 2.08 times the steel model BS.

3.3. *Comparison of test results and analysis*

Bending strength of CFIG was analytically obtained by dividing the cross-section into fibres and compared with the experimental results (Fig.11). The calculated bending strength of CFIG is nearly the same as the BC-N model. As the vertical reinforcing bars are not welded to the flanges of steel girder in BC-N, the confined effects of concrete decreased and the bending strength is smaller than BC by 15 %.

The vertical reinforcing bars are not welded to the flanges of steel girder in BC-N but welded in BC. This is the only difference between BC and BC-N, and causes the difference of bending strength. It would suggest that the confined effects of concrete is larger in BC. Another reason would be that the load transfer mechanism would exist in BC such as Vierendiel Truss effect would exist in BC. Further study must be essential to clarify these ideas.

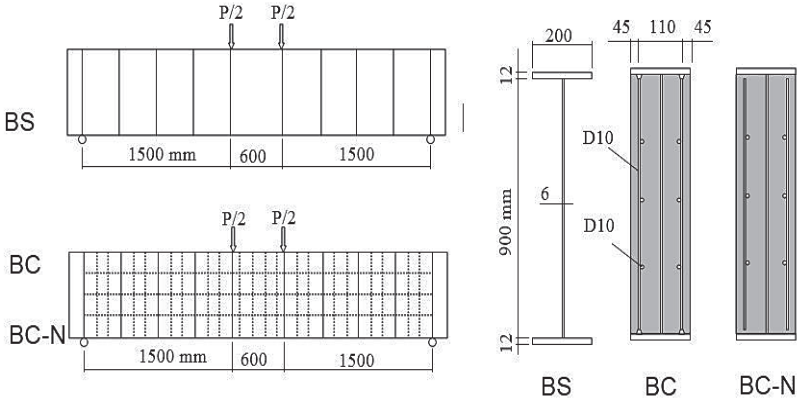

Fig.9 Bending test models

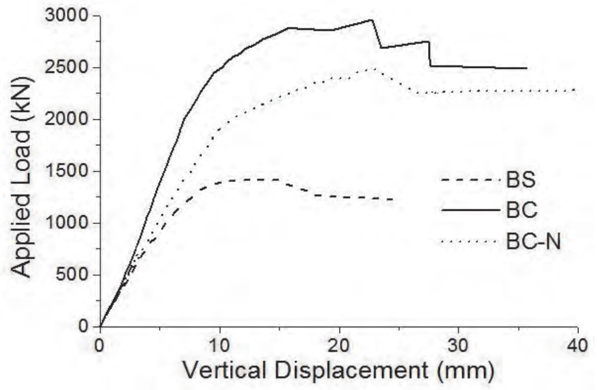

Fig.10 Applied load vs. vertical displacement

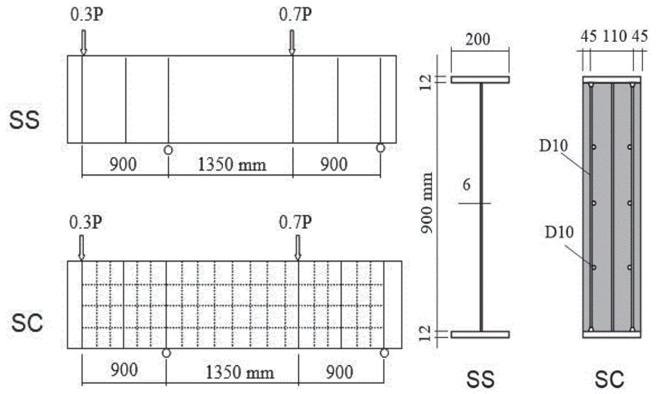

Fig.12 Test method and models of shear test

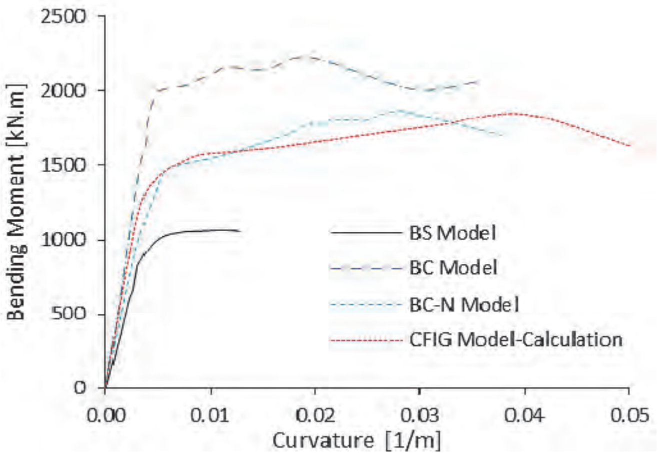

Fig.11 M-ø relation of the experiment & calculation

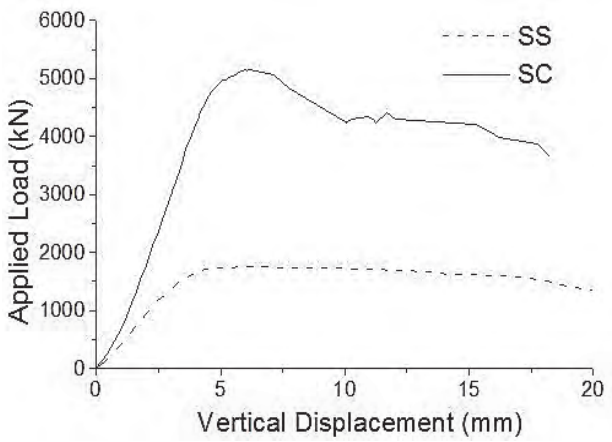

Fig.13 Measured vertical displacement in shear test

4. Shear Test

4.1 *Test method and specimens*

The shear strength of the CFIG was studied. The shear test method and samples are shown in Fig.12. Two models were tested. The model SS is the steel girder model, where the first S stands for shear and the second S for steel. The model SC is the concrete encased steel girder, where C stands for concrete.

The steel girder had the same dimension as the bending test models with a yield stress of 372.3 MPa and a tensile strength of 511.4 MPa. The model was supported at two points at a distance of 1350 mm and had a cantilever section with a length of 900 mm. The shear panel was 1350 mm long and 900 mm high, giving the aspect ratio of 1.5. The girder model was loaded at the cantilever end and at the boundary of the shear panel, so that the shear force was dominant in this shear panel.

The vertical reinforcing bar was 10 mm in diameter and installed at intervals of about 200 mm. The horizontal reinforcing bars were also installed on three vertical levels. Concrete was poured in the same way as the bending models. The compressive strength of concrete was 55 MPa, which was obtained by the test samples.

4.2. *Test result*

Fig.13 shows the measured vertical displacements of the two models at the loading position in the center span. In SS, the vertical displacement increased linearly with the applied load in the elastic stage, but the load decreased after the web buckled. However, since the tension field action appeared in the diagonal direction after the web buckled, the displacement continued to increase.

In SC, the vertical displacement also increased linearly with the applied load in the elastic stage. Cracks appeared on the concrete surface at the applied load of 1000 kN but did not develop afterwards. The encased composite model SC had superb shear strength. The maximum load reached three times that of the steel model SS and the elastic modulus was also much higher.

The load transfer mechanism would be as follows. Shear forces are resisted by the tension strut and the compression strut which act in the diagonal direction, which forms the truss structure. The tension strut is caused by the steel web and the compression strut is caused by the filled concrete. The design formula could be obtained considering this truss action but further study is necessary to established.

5. Conclusions

A new steel/composite girder was proposed and applied to continuous girder bridge. The area surrounded by the flanges and the web is filled with concrete of the CFIG model at the intermediate support.

A trial design was carried out for the four-span continuous highway bridge with span of 43+53+53+43 m. The result with the CFIG was compared with CCG (conventional composite girder), which showed that the thickness of the flanges and web of CFIG can be less than 70% at the intermediate support and 10 % at the mid span of the bridge of CCG.

Bending tests were performed with CFIG and CCG. The maximum bending strength of the filled concrete model was 2.08 times the conventional steel model. The calculation method was proposed for bending strength of CFIG, which agreed with those obtained by experiment.

Shear tests were also performed with CFIG and CCG. The shear strength of CFIG was three times that CCG, showing superb shear resistance against. Truss action with the tension strut of the steel web and the compression strut of the filled concrete may exist, which will be verified by the future study.

This study shows that the proposed concrete filled steel I-girder is feasible and economical compared with the conventional plate girder bridge.

References

1) Nakamura, S., Momiyama, Y., Hosaka, T. and Homma, K.: New technologies of steel/concrete composite bridges, Elsevier, Journal of Constructional Steel Research, Vol.58, pp.99-130, 2002.
2) Nakamura, S. and Narita, N: Bending and shear strengths of partially encased composite I-girders, Elsevier, Journal of Constructional Steel Research, Vol.59, 2003, pp.1435-1453, 2003.
3) Japan Road Association: Specifications for highway bridges, I. General, II. Steel Bridges, 2014
4) Japanese Association of Civil Engineers: Guidelines for performance verification of steel–concrete hybrid structures, 2006.